Liquid water infiltration into a layered snowpack: evaluation of a 3D water transport model with laboratory experiments

Hiroyuki Hirashima[1], Francesco Avanzi[2], Satoru Yamaguchi[1]

[1]Snow and Ice Research Center, National Research Institute for Earth Science and Disaster Resilience, Suyoshi-machi,
Nagaoka-shi, Niigata-ken, 940-0821, Japan
[2]Department of Civil and Environmental Engineering, Politecnico di Milano, Milano, Italy

Correspondence to: Hiroyuki Hirashima (hirasima@bosai.go.jp)

Abstract. The heterogeneous movement of liquid water through snowpack during precipitation and snowmelt leads to complex liquid water distributions that are important for avalanche and runoff forecasting. We reproduced the formation of capillary barriers and the development of preferential flow through snow using a multi-dimensional water transport model, which was then validated using laboratory experiments of liquid water infiltration into layered, initially dry snow. Three-dimensional simulations assumed the same column shape and size, grain size, snow density, and water input rate as the laboratory experiments. Model evaluation focused on the timing of water movement, the thickness of the upper layer affected by ponding, and on water content profiles and the wet snow fraction. Simulation results showed that the model reconstructs some relevant features of capillary barriers including ponding in the upper layer, preferential infiltration far from the interface, and the timing of liquid water arrival at the snow base. In contrast, the area of preferential flow paths was usually underestimated and consequently the averaged water content in areas characterized by preferential flow paths was also underestimated. Improving the representation of water preferential infiltration into initially dry snow is necessary to reproduce the transition from a dry-snow-dominant condition to a wet-snow-dominant one, especially in long-period simulations.

1 Introduction

The heterogeneous movement of liquid water through snowpack during precipitation and snowmelt leads to complex liquid water distributions that impact on snow structure through wet snow metamorphism. Furthermore, grain growth and subsequent changes in pore sizes and pore size distribution under wet conditions decrease snow strength (Wakahama, 1968; Raymond and Tsushima, 1979; Colbeck, 1983; Brun and Ray, 1987; Marsh, 1987; Brun et al. 1989; Lehning et al., 2002; Yamanoi and Endo, 2002; Ito et al., 2012) and can lead to wet snow avalanches (Kattelmann, 1984; Fierz and Föhn, 1994; Baggi and Schweizer, 2008; Mitterer et al. 2011; Mitterer and Schweizer, 2013; Takeuchi and Hirashima, 2013; Wever et al.,

2016a). Liquid water movement through the snowpack also controls the lag between rain events or snowmelt and water arrival at the snow base.

In the early theories of liquid water movement, capillary gradients in snow were usually neglected (Colbeck, 1972; Colbeck and Davidson, 1972; Colbeck, 1974b, 1976; Dunne et al., 1976; Wankiewicz, 1978). For example, Marsh and Woo (1985)

5   developed a model of flow channels but neglected the gradient term of capillary pressure. A two-dimensional (2D) model by Illangasekare et al. (1990) considered the gradient of capillary pressure, but focused on the effects of ice layers without considering the dependency of capillary pressure on grain size and density. A 2D model by Daanen and Nieber (2009) adopted a van-Genuchten model with dependence on grain size. For each of these models, the main cause of heterogeneous water movement was attributed to refreezing and ice layers. In porous media (e.g., soil), water can pond owing to capillary

10 barrier, which consequently delays infiltration (e.g. Clifford and Stephen, 1998; Kämpf et al, 2003); however, water can also pond and consequently form preferential flow in layered snow, even when no ice layer forms (Waldner et al., 2004; Katsushima et al., 2013; Avanzi et al., 2016).

Capillary barriers form owing to differences in the matrix potential between layers. Hirashima et al. (2010) replicated capillary barrier formation in the SNOWPACK model using parameters of matrix potential obtained from gravity drainage

15 column experiments performed by Yamaguchi et al. (2010). Wever et al. (2014) incorporated the Richards Equation into the SNOWPACK model and obtained a good correlation with observed runoff. They also compared upGPR data with lysimeter data and showed that, even if the simulated waterfront did not arrive at the snow base, runoff was still initiated. This was interpreted to reflect the effect of preferential flow, which was not included in the model (Wever et al., 2015).

More recent studies have modelled preferential flow; for example, Katsushima et al. (2013) used laboratory experiments in

20 vertically homogeneous snow to show that water entry suction, which in turn is related to grain size, affects the formation of preferential flow. On the basis of this work, Hirashima et al. (2014a) developed a three-dimensional (3D) water transport model for snowpack that is able to reproduce preferential flow as a function of water entry suction and validated it using the results of Katsushima et al. (2013). However, as snowpack contains multiple layers of snow with different densities and grain sizes, simulations and laboratory experiments of water infiltration for different snow layers remain necessary.

25 Furthermore, because simulation results for multiple-layer snow have not yet been validated using real data (Hirashima et al., 2013; Hirashima et al., 2014b), the accuracy of the model remains uncertain. Avanzi et al. (2016) performed an infiltration experiments for multi-layered snowpack with different combinations of grain size and infiltration rate and measured liquid water distribution, thickness of the capillary barrier, and arrival time.

Recently, a dual domain approach has been suggested to consider preferential flow effects in one-dimension (1D; Wever et

30 al., 2016b; Würzer et al. 2017); however, considering a heterogeneous processes in 1D model requires several assumptions. Simulations of multi-dimensional water transport models and laboratory experiments can provide the data needed to develop exhaustive parameterization of 3D processes for 1D models. In this study, simulations of liquid water infiltration into layered snowpack were performed by reproducing the laboratory experiments of Avanzi et al. (2016). The purpose of this study was: (1) to evaluate the accuracy of a 3D water transport model in reproducing infiltration patterns in layered snow; (2) to gain

further insight into the 3D infiltration process into layered snow by comparing simulation results with data from laboratory experiments; and (3) to identify future avenues of development for 3D water transport schemes in snow.

2 Simulation method

2.1 Model

Details of the multi-dimensional water transport model are provided in Hirashima et al. (2014a). Models of liquid water movement in porous media use the Richards' equation and the Darcy-Buckingham law, which require knowledge of capillary pressure gradients and hydraulic conductivity. However, while the equation parameters depend on porosity, pore shape, pore connectivity, size distribution, and tortuosity, they are frequently estimated from a combination of snow density and grain size (Jordan et al., 2008). In the multi-dimensional model used here (Hirashima et al., 2014a), the relationship between capillary pressure, water content, grain size, and snow density (the so-called water retention curve) was determined based on gravity drainage column experiments performed by Yamaguchi et al. (2012). The relationship between saturated hydraulic conductivity, snow density, and grain size was estimated from the results of Calonne et al. (2012), who considered snow microstructure using the equivalent sphere radius estimated from specific surface area (instead of grain size). We considered grain size to be equal to equivalent sphere radius (Hirashima et al., 2014a). Unsaturated hydraulic conductivity was estimated using the van Genuchten-Mualem model (Mualem, 1976; van Genuchten, 1980). Water entry suction, which is necessary to reproduce preferential flow (Hirashima et al., 2014a), was measured and formulated as a function of grain size following the approach of Katsushima et al. (2013).

2.2 Comparative simulation

Hirashima et al. (2014a) performed infiltration simulations within columns with only one layer of snow. A number of multi-layer simulations were also tested (Hirashima et al, 2013, 2014b); however, they were performed in 2D and were not validated with observations. In this study, validation of the water transport model for layered snow was performed using observations of infiltration patterns performed using dye trace experiments (Avanzi et al., 2016). In these experiments, snow was packed in a cylindrical container composed of several acrylic rings (height equal to 20 mm, diameter equal to 50 mm). Nine or ten acrylic rings were stacked to store 10 cm of upper layer snow and 8 or 10 cm of lower layer snow. All samples were characterized by finer-over-coarser layering (i.e., the upper layer was created using a smaller grain size than the lower layer), which aimed to reproduce capillary barriers. Three types of snow grain size included fine (0.25–0.5 mm), medium (1.0–1.4 mm), and coarse (2.0–2.8 mm). While this definition is convenient for the scope of this study, it is not consistent with the International Classification proposed by Fierz et al. (2009). Three water input rates were considered, (10 mm/h, 30 mm/h, and 100 mm/h). In total, 9 experiments were performed (i.e., one for each grain size/input rate combination).

3D simulations had dimensions of 5, 5, and 20 cm in the x, y, and z directions, respectively. The voxels were 5 mm on the sides. Voxels of more than 2.5 cm from the central axis were treated as an impermeable wall, which ensured that the simulated shape was columnar. Snow densities, grain sizes, and rates of water supply were set to the same values as in the laboratory experiments. Grain size distributions were not measured: instead, for fine and medium snow we used the median

5   grain sizes obtained by Katsushima et al. (2013) using the same sieves (0.406 and 1.463 mm, respectively). Grain size for coarse snow was determined assuming it as two times the median medium grain size (2.926 mm). As a measurement of horizontal structural heterogeneity, we estimated the standard deviation following the approach of Hirashima et al. (2014a), who estimated that the standard deviation of grain size is 20% of the median grain size (Katsushima et al., 2013). In this simulation, heterogeneity of snow density was not provided. As with the cases of laboratory experiments, grain size

10   combinations in the simulation were fine-over-coarse snow (FC), fine-over-medium snow (FM), and medium over coarse snow (MC). Values of snow density and water supply rates are shown in Table 1.

The evaluation of simulations focused on the thickness of the ponding layer at the textural interface, on the liquid water distribution, on the wet snow fraction at different heights, and on the timing of water arrival at the interface between layers, of breakthrough of preferential flow in the lower layer, and of arrival of liquid water at sample base. Data of liquid water

15   content, wet snow fraction, and thickness of the ponding layer were measured by Avanzi et al. (2016), whereas timings were obtained from available video recordings of the experiments. A small difference (mean of 0.5 minutes, maximum of 3 minutes for FC1) was found between the arrival times from video recordings and those in Avanzi et al. (2016); data from videos were used here for consistency with the other timings (see Table 2). The simulated timings of water arrival at the interface, entering the lower layer, and arrival at the snow base refer to the lowest meshes in the upper layer, the top 3

20   meshes in lower layer, and the lowest meshes of the sample, respectively. The water content in the top 3 meshes of the lower layer was used to determine the timing of breakthrough because preferential flow expended immediately after the water content of one of these meshes became larger than zero.

3 Simulation results

3.1 Water percolation through preferential flow path and capillary barrier

As an example, some images of the development of capillary barrier and preferential flow for FC1 are shown in Fig. 1. These figures show the front surfaces after 20 sec from the beginning of the experiment (a and e), at the arrival time of water at the interface between layers (b and f), at the time of breakthrough of preferential flow into the lower layer (c and g) and at the arrival time at the snow base (d and h). The simulation results showed faster than anticipated arrival of water at the

30   boundary (Table 2), which implied an overestimation of vertical velocity in the model's preferential flow for this experiment (Fig. 1). In Figs. 1b and 1f, elapsed times were indeed 35 and 17 minutes in the laboratory experiment and simulation, respectively. One possible cause is the underestimation of the area of preferential flow path, which was also considered by

Hirashima et al. (2014a). A smaller path area would increase conductivity because liquid water would be more concentrated and push water towards the boundary faster. After arrival at the boundary, we found that liquid water ponded above the boundary owing to a capillary barrier. In images from just before the formation of preferential flow in the lower layer (Fig. 1c and g), the elapsed time was 85 in the laboratory experiment and 79 minutes in the simulation (relative difference of 7% of the measurement value, i.e., in good agreement).

The times of liquid water arrival at the base following the formation of preferential flow through the lower layer were 4 and 1 minutes in the laboratory experiment and simulation, respectively. On this basis, we calculated the propagation rate of the preferential flow path to be 0.4 and 1.6 mm/s for the laboratory experiment and simulation, respectively. This is one order of magnitude smaller than mean speed of preferential flow (11.2 mm/s) measured by Walter et al. (2013) using fluorescent particle tracking velocimetry; however, this was tested with a much larger water supply rate (3600 mm/h).

In the other experiments, the temporal dynamics of preferential flow formation and water ponding at the interface were generally well reproduced (Table 2; Fig. 2). The Root Mean Square Error, the slope of a regression line with intercept equal to 0, and the correlation coefficient (r^2) between the simulated and measured timings were 7.8 min., 0.97 and 0.93, respectively. As timings were measured using frontal movies, we were sometimes unable to evaluate the timing of preferential flow formation within a sample (e.g., experiment MC1); therefore, estimated timings from laboratory experiment may contain a delay. Overall, simulated and measured timings coincided well, which confirms that if snow parameters (e.g., snow density and grain size) are known, the arrival time of liquid water can be predicted using this model.

3.2 Thickness of water ponding layer

Avanzi et al. (2016) measured the thickness of the upper layer affected by ponding at the end of each experiment. In their results for FC and FM experiments, the liquid water content on the layer boundary was about 33–36% (2-cm vertical resolution of data). The volume of ponded water was smaller for MC experiments. Laboratory experiments confirmed that the thickness of the water ponding layer is not strongly connected to the water input rate. Here, the influence of water input rate on the thickness of water ponding layer was also small; however, the influence of grain size was significant (Table 3).

The thickness of ponded water at the interface was well reproduced for the FC experiments, but was overestimated for FM experiments and underestimated for MC experiments. For MC experiments, up to 1 cm of ponding was shown in laboratory experiments, while simulated results showed a thickness of less than 0.5 cm.

3.3 Horizontal cross section

During laboratory experiments, Avanzi et al. (2016) measured wet snow fractions at the boundary between consecutive rings using photos of the top surface of the ring below the boundary. Samples were likely slightly compressed during experiments (Marshall et al. 1999), even though this was not noticeable. Because the model does not include settling, we chose to

compare data with simulations of the inferior surface of the ring above the boundary, which returned more consistent results. At the interface between layers, most of the area of each section was wet, except for the medium over coarse samples (Fig. 3). For the other sections, only a fraction was found to be wet. This pattern was well simulated (Fig. 4); although simulated wet snow areas were smaller than those measured especially in areas characterized by preferential flow. Similar

5   underestimation by the model was also observed by Hirashima et al. (2014a).

3.4 Water content distribution

Our simulations were performed with 5 mm voxels. Simulated water contents from all voxels at a given height were averaged to obtain the water content profile. In laboratory experiments, water content profiles were obtained with a

10   resolution of 2 cm (Fig. 5). The results showed that for the FC and FM experiments, the liquid water content was overestimated near the interfaces between snow layers in the upper fine layer but underestimated in other areas. The impact of water supply rate on the water content in capillary barriers was small in both simulations and experiments. Overall, simulations and observations showed good agreement in that liquid water content increased with depth in the finer layer, peaked at the interface between layers, and decreased in the lower layer.

4 Discussion

4.1 Comparison with a matrix-flow multi-layer model

The numerical snowpack model SNOWPACK can also be used to reproduce dynamics observed during laboratory

20   experiments. While Avanzi et al. (2016) compared their results with SNOWPACK-3.3.0 simulations at the end of each experiment (i.e. at the observed/modelled arrival time of water at the snow base), the comparison between models can be made for any point of time. Here, we compared temporal changes in the simulated water content profiles for SNOWPACK and the 3D model in order to assess the role played by a simulation of preferential flow in controlling liquid water distribution in snow (Fig. 6; Fig. S1); therefore, we chose an approach that did not consider preferential flow as a benchmark

25   (i.e., the matrix-flow multi-layer implementation of the Richards Equation in SNOWPACK; Wever et al., 2015).

In the SNOWPACK simulations, liquid water content in the upper layer gradually increased with time at all the positions (Fig. 6; Fig. S1), and the water content near the boundary was relatively large. The difference in water content between the layer interfaces and the upper part was underestimated when compared with experimental results, which confirm a marked spatial heterogeneity in liquid water distribution. On the other hand, 3D simulation showed that liquid water quickly ponds at

30   the boundary, which is consistent with the experimental observations. Such an effect is obtained thanks to preferential flow, which allowed water to move in small fingers and to reach deeper locations, even when most of the upper snow remained

dry. The water ponding layer thickened until the formation of a preferential flow path in the lower layer. The difference in water content between layer interfaces and the upper part was overestimated in comparison with the experimental observations.

For arrival times, the 3D model obtained greater accuracy than the SNOWPACK simulations, which again suggests the

5   importance of considering preferential flow. Causes of delay in 1D models include both slow infiltration of matrix flow and overestimation of water ponding at the capillary barrier (Fig. 6). A more detailed comparison of arrival times between models will be, however, the object of a future study that includes the dual-domain approach, which considers preferential flow in 1D; this process is expected to play a key role for arrival times.

The theory of water transport in the SNOWPACK model is based on gravity drainage column experiments that neglect

10   water entry suction (i.e., experiments performed using wet snow; Yamaguchi et al., 2012). In contrast, the 3D model includes an attempt to simulate the infiltration process into initially dry snow using water entry suction (where we define dry snow as that with a lower liquid water content than the irreducible water content), which is key to reproducing fingers (Hirashima et al., 2014a). Under these conditions, the van Genuchten model could only be used with additional assumptions (Hirashima et al., 2014a). Accordingly, we assumed that dry snow had a threshold suction equal to water entry suction.

15   Future work will focus on improving this approach; for example, water entry suction may be related to the suction – wetness profile of a wetting water retention curve (Avanzi et al., 2016), which has not yet been parameterized. Furthermore, unsaturated conductivity tends towards zero in dry conditions, but extensive observations of unsaturated conductivity in snow are missing.

20   **4.2 Wet snow ratio in preferential flow path area.**

In practice, the main purpose of the development of this model is to include 3D patterns of water infiltration in snow and, thus, resolve the delay of the arrival time as a limitation of matrix-flow models (see the previous section). The simulation results showed that the model can reproduce preferential flow and capillary barriers and, consequently, provide reliable estimations of the arrival time of water at sample base. On the other hand, it underestimated the simulated preferential flow

25   area. In terms of effect on arrival time, this underestimation is not a serious problem because the travel time through the preferential flow area was short (Table 2); however, it may represent a problem for long-term simulations, especially when estimating the transition from a predominantly dry snow to a predominantly wet snow.

According to the simple model of Baker and Hillel (1990), the wetted fraction of the sublayer in a finer-over-coarser transition depends on water input rate and unsaturated conductivity during steady vertical infiltration. Horizontal expansion

30   of preferential flow also depends on infiltration along the horizontal direction. As the direction of water flow depends on gravity (vertical) and capillarity, movement in the horizontal direction may be impeded if simulated capillary gradients are small. For example, the fact that fine snow in experiments had the larger preferential flow paths than coarse snow was probably due to a greater difference in capillarity by heterogeneity (Avanzi et al., 2016).

We performed sensitivity tests to estimate the relevance of vertical and horizontal movement for different types of snow, in which we calculated which voxel (left, right, front, back, up, down) was easiest to infiltrate from a generic voxel as a function of gravity or water entry suction. We found that the ratio of the water moving to the lower voxel was 24.3%, 38.8% and 60.7% for fine, medium and coarse snow, respectively. When this ratio is large (e.g., coarse snow), water moves

5   downward, and consequently the preferential flow path areas become small. Where there is no gravitational force, the ratio would be 16.7% while for fine snow the ratio of water moving to the lower voxel was 24.3%. Nevertheless, the simulated mean wet snow area was not large even for the fine snow (e.g. 4.8% in FC1 and 22% in FC3, excluding the ponding area). These results suggest that infiltration for dry snow is too vertically strict in this version of the model.

In this model, water entry suction was used as threshold for liquid water infiltration into dry snow. However, in the measured

10   water absorption curve of Adachi et al. (2012), the relationship between suction and liquid water content was non-linear and hysteretic (see Section 4.1). This simplified condition for infiltration into dry snow may lead to an underestimation of the expansion of preferential flow. The number of preferential flow paths can also promote the expansion of the wet snow area (Schneebeli, 1995). In our model, liquid water preferred to infiltrate snow along the same path; therefore, preferential flow paths did not increase unless the amount of liquid water supply also increased. Also, compaction by wet snow

15   metamorphism could change the balance of force distribution and create new pathways for liquid water. This underestimation may also be related to uncertainties in the computation of unsaturated water conductivity in initially dry snow and/or in the rule used to calculate the conductivity between voxels. New techniques to measure the development of preferential flow paths can help to model these processes and further experiments in this direction are, therefore, highly needed.

4.3 Outlook

Recently, a dual domain approach has been developed to consider the effects of preferential flow in 1D models (Wever et al., 2016b; Würzer et al., 2017). While this approach has proven useful for avalanche prediction and hydrological simulations, some assumptions are needed to model heterogeneous processes using 1D models. As these assumptions are aimed at

25   parameterizing 3D processes in 1D, the 3D model developed here represents an important stage in model development. However, the low accuracy of preferential flow path area in our model means that it cannot be used to improve the parameterization of preferential flow area as of Wever et al. (2016b). In the future, a more exhaustive parameterization of hysteresis in snow and the a better reconstruction of the expansion of preferential flow path area will improve the accuracy of 3D models and allow for an advanced estimation of preferential flow area in 1D models. Wever et al. (2016b) also

30   suggested that 3D models should analyse heat exchange around the preferential flow path; therefore, future developments of our model will consider heating and melt-freeze processes (e.g., the model of Leroux and Pomeroy [2016]). For this, laboratory experiments of ice layer formation will be needed for validation.

Another possible improvement to the model would be the parameterization of quick grain growth at saturation, which would be necessary for simulating the structural evolution of areas affected by ponding. Grain growth causes an abrupt decrease in suction and consequently reduces the water content at the ponding layer. The water content of the upper layer at 2t was smaller than that at 5t/3 (Fig. 6a, t is the measured arrival time) owing to a decline of suction due to grain growth. In the first

5   version of SNOWPACK model, the Brun et al. (1989) equation was used for estimating grain growth; however, this formula is based on data with small water content and application to saturated conditions may overestimate grain growth. To avoid this, Hirashima et al. (2010, 2014a), used the equation of Tusima (1978) to constrain the upper limit of grain growth rate. Although this formula is based on data measured under saturated conditions, grain growth remains limited for a short time scale such as these experiments. The grain growth equation of Tusima (1978) was formulated using data for 200 hours, but it

10   did not focus on the first 1 hour; therefore, grain growth over short time periods and under saturated condition remains unclear. Raymond and Tusima (1979), Wakahama (1968), and Colbeck (1973) all focused on wet snow metamorphism under saturated conditions, but they also did not focus on the first hour of the experiments. Extending the existing parameterizations of wet snow metamorphism for small timescales will improve simulation accuracy with regards to the development and disappearance of water ponding by capillary barriers.

5 Conclusions

Validation of simulations for capillary barrier formation and subsequent preferential flow development was performed using a multi-dimensional water transport model. Overall, the infiltration process into dry snow was well reproduced, and in

20   particular the timing of liquid water arrival at the snow base was accurate. A detailed comparison of wet conditions in the snow column was performed to check accuracy and identify shortcomings in the model. The model accurately reproduced: (a) the onset of preferential flow in initially dry snow; (b) the ponding of liquid water above the boundary of snow layers by capillary barrier, for which the ponded water volume was larger at the boundary of fine over coarse and fine over medium snow layers than it was at the boundary of medium over coarse snow layers.

25   Model discrepancies included: (a) an underestimation of liquid water content and wet snow area in preferential flow path areas, and (b) overestimation of water ponding volume at the layer boundary in experiments FC and FM, but underestimation in experiment MC. Future improvements to the model will include improving the water entry process for dry snow, measurements of water content profile for capillary rise, and direct measurements of preferential flow path formation. The advantage of this model over 1D models is the consideration of 3D heterogeneous infiltration into dry snow. An explicit

30   simulation of preferential flow also returns a reliable estimation of liquid water arrival at the snow base. However, improvements are needed to ensure that the model works over both long and short time periods. An accurate reproduction of the transition from a dry-snow dominant to a wet-snow dominant condition is an important step in upgrading this model to a full 3D numerical snowpack model.

Acknowledgement

This study was part of the "Research on Advanced Snow Information and its Application to Disaster Mitigation" project, and was supported by JSPS, KAKENHI Grant Numbers JP15H01733. Fruitful discussions about this work with Y. Ishii and T.

5   Katsushima are acknowledged. We thank the members of the Snow and Ice Research Center for their advice and discussion. We are grateful to M. Miura, who assisted with our research.

References

Adachi, S., Yamaguchi, S., Ozeki, T., and Kose, K.: Hysteresis in the water retention curve of snow measured using an MRI
10   system, Proceedings, International Snow Science Workshop, Anchorage, Alaska, 918-922, 2012.

Avanzi, F., Hirashima, H., Yamaguchi, S., Katsushima, T., and De Michele, C.: Observations of capillary barriers and preferential flow in layered snow during cold laboratory experiments, The Cryosphere, 10 (5), 2013–2026, doi:10.5194/tc-10-2013-2016.

Baggi, S. and Schweizer, J.: Characteristics of wet-snow avalanche activity: 20 years of observations from a high alpine
15   valley(Dischma, Swizerland), Natural Hazards, 50, 97-108, 2008.

Brun, E., Martin, E., Simon, V., Gendre, C., and Coleou, C.: An energy and mass model of snow cover suitable for operational avalanche forecasting, J. Glaciol., 35, 333–342, 1989.

Brun, E., and Ray, L.: Field study on snow mechanical properties with special regard to liquid water content, in Avalanche formation, movement and effects, Proceedings of the Davos Sympsium, September 1986, IAHS, publ, 162, 1987.

20   Calonne, N., Geindreau, C., Flin, F., Morin, S., Lesaffre, B., Rolland du Roscoat, S., and Charrier, P.: 3-D image-based numerical computations of snow permeability: links to specific surface area, density, and microstructural anisotropy, The Cryosphere, 6, 939–951, doi:10.5194/tc-6-939-2012, 2012.

Clifford K. H. and Stephen W. W.: Capillary barrier performance in heterogeneous porous media, Water resources research, 34, 603-609, 1998.

25   Colbeck, S. C.: A theory of water percolation in snow, J. Glaciol., 11, 369–385, 1972.

Colbeck, S. C. and Davidson, G.: Snow percolation through homogeneous snow, in: Int. Symp. on the Role of Snow and Ice in Hydrology, Banff, AB, Canada, 1972.

Colbeck S. C.: Theory of metamorphism of wet snow, CRREL Res. Rep. 313, 1973

Colbeck, S. C.: The capillary effects on water percolation in homogeneous snow, J. Glaciol., 13(67), 85–97, 1974a.

30   Colbeck, S. C.: Water flow through snow overlying an impermeable boundary, Water Resour. Res., 10, 119–123, doi:10.1029/WR010i001p00119, 1974b.

Colbeck, S. C.: An analysis of water flow in dry snow, Water Resour. Res., 12, 523-527, doi:10.1029/WR012i003p00523, 1976.

Colbeck, S. C.: Theory of metamorphism of dry snow, J. Geophys. Res., 88, 5475-5482, 1983.

Daanen, R. P. and Nieber, J. L.: Model for Coupled Liquid Water Flow and Heat Transport with Phase Change in a Snowpack, J. Cold Reg. Eng., 23, 43–68, 2009.

Dunne, T., Price, A.G., and Colbeck, S.C.: The Generation of Runoff From Subarctic Snowpacks, Water Resour. Res., 12, 677-685, 1976.

Fierz, C. and Fo˙hn, Paul M. B.: Long-Term observation of the water content of an alpine snowpack, Proceedings of the International Snow Science Workshop; Snowbird, Utah, USA; pp. 117-131, 1994.

Fierz, C., Armstrong, R. L., Durand, Y., Etchevers, P., Greene, E., McClung, D. M., Nishimura, K., Satyawali, P. K., and Sokratov, S. A.: The International Classification for Seasonal Snow on the Ground, Tech. rep., IHP-VII Technical Documents in Hydrology N 83, IACS Contribution N 1, UNESCO-IHP, Paris, 2009.

Kämpf, M., Holfelder, T. and Montenegro, H.: Identification and parameterization of flow processes in artificial capillary barriers, Water Resour. Res., 39, doi:10.1029/2002WR001860, 2003.

Hirashima, H., Yamaguchi, S., Sato, A., and Lehning, M.: Numerical modeling of liquid water movement through layered snow based on new measurements of the water retention curve. Cold Reg. Sci. Technol., 64, 94-103, doi:10.1016/j.coldregions.2010.09.003, 2010.

Hirashima, H., Yamaguchi, S. and Katsushima, T.: A multi-dimensional water transport model to reproduce preferential flow in the snowpack, International Snow Science Workshop Grenoble-Chamonix Mont-Blanc, 31-37, 2013.

Hirashima, H., Yamaguchi, S. and Katsushima, T.: A multi-dimensional water transport model to reproduce preferential flow in the snowpack, Cold Reg. Sci. Technol., 108, 80–90, 2014a.

Hirashima, H., Yamaguchi, S., and Ishii, Y.: Simulation of liquid water infiltration into layered snowpacks using multi-dimensional water transport model, ISSW proceedings, Banff, 48-54, 2014b.

Illangasekare, T.H., Walter, Jr., R.J., Meier, M.F., and Pfeffer, W.T.: Modeling of meltwater infiltration in subfreezing snow. Water Resour. Res., 26, 1001-1012, doi:10.1029/WR026i005p01001, 1990.

Ito, Y., Matsushita, H., Hirashima, H., Ito, Y., and Noro, T.: Change in snow strength caused by rain, Ann. Glaciol, 53 (61), 1–5, 2012.

Jordan, R., Albert, M.R., and Brun, E.: Physical processes within the snow cover and their parameterization. In: Armstrong, R., Brun, E. (Eds.), Snow and Climate. Cambridge University Press, 12–69, 2008.

Katsushima, T., Yamaguchi, S., Kumakura, T., and Sato, A.: Experimental analysis of preferential flow in dry snowpack, Cold Reg. Sci. Technol., 85, 206-216, doi:10.1016/j.coldregions.2012.09.012, 2013.

Kattelmann, R.: Wet slab instability, in: Proceedings of the 1984 International Snow Science Workshop, 102-108, 1984.

Lehning, M., Bartelt, P., Brown, B., Fierz, C., and Stayawali, P.: A physical SNOWPACK model for the Swiss avalanche warning Part II. Snow microstructure, Cold Reg. Sci. Technol., 35, 147-167, 2002.

Leroux, N. R. and Pomeroy, J. W.: A 2D model for simulating heterogeneous mass and energy fluxes through melting snowpacks, The Cryosphere Discussion, doi:10.5194/tc-2016-55, 2016.

Marsh, P., and Woo, M.: Meltwater movement in natural heterogeneous snow covers, Water Resour. Res., 21, doi:10.1029/WR021i011p01710, 1710-1716, 1985.

5   Marsh, P.: Grain Growth in a wet arctic snow cover, Cold Reg. Sci. Technol., 14, 23-31, 1987.

Marshall, H.P., Conway, H., Rasmussen, L.A.: Snow densification during rain. Cold Reg. Sci. Technol., 30, 1-3, 35-41, doi: 10.1016/S0165-232X(99)00011-7, 1999.

Mitterer, C., Hirashima, H., and Schweizer, J.: Wet-snow instabilities: comparison of   measured and modelled liquid water content and snow stratigraphy, Ann. Glaciol., 52, 201–208, 2011.

10 Mitterer, C. and Schweizer, J.: Analysis of the snow-atmosphere energy balance during wet-snow instabilities and implications for avalanche prediction, The Cryosphere, 7, 205 – 216, 2013.

Mualem, Y.: A new model for predicting the hydraulic conductivity of unsaturated porous media, Water Resour. Res., 12, 513-522, 1976.

Raymond, C. F. and Tsushima, K.: Grain coarsening of water-saturated snow, J. Glaciol. 22, 83-105, 1979.

15 Schmid, L., Koch, F., Achim, H. Monika, P., Olaf, E., Wolfram,M., and Jürg, S.: A novel sensor combination (upGPR-GPS) to continuously and nondestructively derive snow cover properties, Geophys. Res. Lett, 3397-3405, 2015.

Schneebeli, M.: Development and stability of preferential flow paths in a layered snowpack, Biogeochemistry of seasonally snow-covered catchments (proceedings of a boulder symposium, July 1995), IAHS Publ., 228, 89-95, 1995.

Takeuchi, Y. and Hirashima, H.: Snowpack estimations in the starting zone of large-scale snow avalanches in the
20 Makunosawa valley, Myoko, Japan, Ann. Glaciol., 54(62), 19-24, 2013.

Tusima, K.: Grain coarsening of ice particles immersed in pure water (in Japanese, with English Abstr.), Seppyo, 40, 155-164, 1978.

van Genuchten, M.Th.: A closed-form equation for predicting the hydraulic conductivity of unsaturated soils, Soil Sci. Soc. Am. J., 44, 892–898, 1980.

25 Wakahama, G.: The metamorphism of wet snow, in: IAHS Publ., 79, 370–379, 1968.

Waldner, P.A., Schneebeli, M., Schultze-Zimmermann, U., and Flühler, H.: Effect of snow structure on water flow and solute transport, Hydrol. Proc., 18, 1271–1290, doi:10.1002/hyp.1401, 2004.

Walter, B., Horender, S., Gromke, C., and Lehning, M.: Measurements of the pore-scale water flow through snow using Fluorescent Particle Tracking Velocimetry, Water Resour. Res., 49, 7448–7456, doi:10.1002/2013WR013960, 2013.

30 Wankiewicz, A.: A review of water movement in snow, in: Modeling of snow cover runoff, edited by Colbeck,
S. C. and Ray, M., U.S. Army Cold Regions Research and Engineering Laboratory, Hanover, New Hampshire, 1978.

Wever, N., Fierz, C., Mitterer, C., Hirashima, H., and Lehning, M.: Solving Richards Equation for snow improves snowpack meltwater runoff estimations in detailed multi-layer snowpack model, The Cryosphere, 8, 257-274, doi:10.5194/tc-8-257-2014, 2014.

Wever, N., Schmid, L., Heilig, A., Eisen, O., Fierz, C., and Lehning, M.: Verification of the multi-layer SNOWPACK model with different water transport schemes, The Cryosphere, 9, 2655-2707, doi:10.5194/tcd-9-2655-2015, 2015.

Wever, N., Vera Valero, C., and Fierz, C.: Assessing wet snow avalanche activity using detailed physics based snowpack simulations, Geophys. Res. Lett., doi:10.1002/2016GL068428, 2016a.

5   Wever N., Würzer, S., Fierz, C., and Lehning, M.: Simulating ice layer formation under the presence of preferential flow in layered snowpacks, The Cryosphere, doi:10.5194/tc-10-2731-2016, 2016b.

Würzer, S., Wever, N., Juras, R., Lehning, M., and Jonas, T.: Modeling liquid water transport in snow under rain-on-snow conditions – considering preferential flow, Hydrol. Earth Syst. Sci., 21, 174101756, doi:10.5194/hess-21-1741-2017, 2017.

Yamanoi, K. and Endo, Y.: Dependence of shear strength of snow cover on density and water content (in Japanese, with

10   English Abstr.), Seppyo, 64, 443-451, 2002.

Yamaguchi, S., Katsushima, T., Sato, A., and Kumakura, T.: Water retention curve of snow with different grain sizes, Cold Reg. Sci. Technol., 64(2), 87–93, doi:10.1016/j.coldregions.2010.05.008, 2010.

Yamaguchi, S., Watanabe, K., Katsushima, T., Sato, A., and Kumakura, T.: Dependence of the water retention curve of snow on snow characteristics, Ann. Glaciol., 53(61), 6-12, 2012.

Table 1: Experimental conditions after Avanzi et al. (2016).

Sample ID	W (mm h^{-1})	ρ_{DU} (kg m^{-3})	ρ_{DL} (kg m^{-3})
FC1	11.9	417	465
FC2	28	449	483
FC3	113	433	470
FM1	11.9	444	484
FM2	27.7	442	487
FM3	110	455	510
MC1	11	472	487
MC2	27.3	498	480
MC3	111	494	478

Table 2: Timings of infiltration process in laboratory experiments and simulations. [a]

experiment ID	experiment			simulation		
	arrival at boundary	preferential flow formation	arrival at snow base	arrival at boundary	preferential flow formation	arrival at snow base
FC1	34.8	85.0	89.0	16.7	79.0	79.7
FC2	15.2	48.5	49.8	8.7	38.7	39.0
FC3	7.1	12.3	14.0	4.0	11.7	12.0
FM1	20.0	79.0	89.5	17.0	72.3	109.0
FM2	11.3	33.3	39.8	10.7	37.3	58.3
FM3	6.7	11.2	13.0	4.3	11.3	15.7
MC1	5.3	-	9.5	9.0	11.0	11.7
MC2	3.0	5.0	8.0	4.7	5.3	5.3
MC3	0.8	2.5	4.5	1.7	1.7	1.7

a. All the timings were retrieved from the video recording of the experiment. '-' represents points where timings could not be

5   extracted from the video recording of the experiment.

Table 3: Thickness of upper layer affected by ponding at the layer boundary.[a]

Sample ID	experiment (cm)	simulation (cm)
FC1	2-3	2.8 (±0.5)
FC2	3-4	4.1 (±0.4)
FC3	2-3	3.3 (±0.5)
FM1	2-3	4.0 (±0.3)
FM2	2-3	4.8 (±0.4)
FM3	1-2	5.1 (±0.3)
MC1	0-1	0.1
MC2	1-1	0.3
MC3	0.5-1	0.3

5 a. For each pixel at the interface between layers, simulated thickness was first determined by computing the number of voxels above with liquid water content (LWC) of >10%. These data were then used to calculate a mean value and its standard deviation.
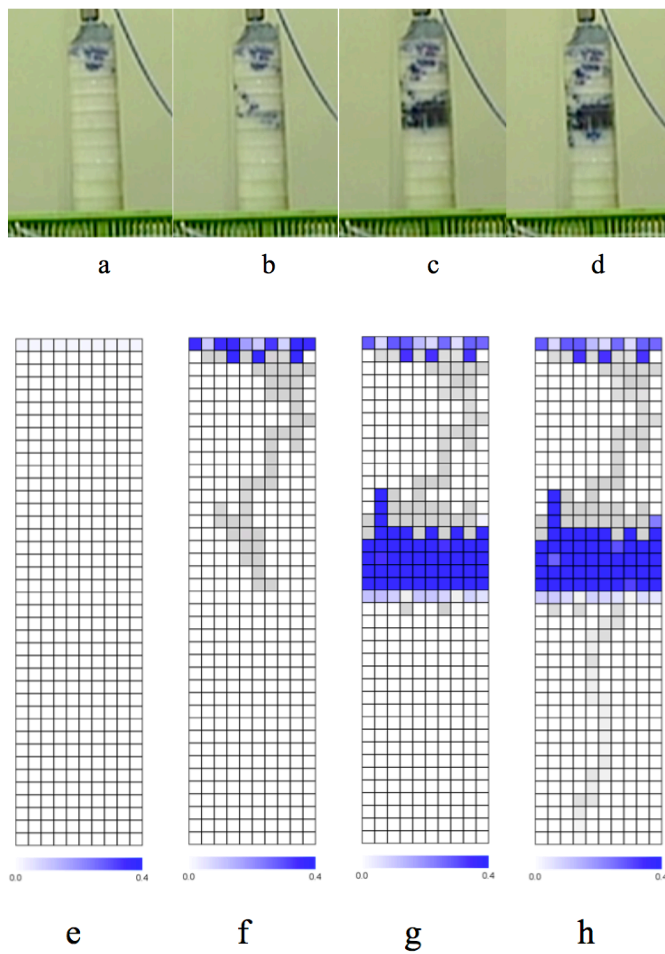
Figure 1: Development of capillary barrier and preferential flow path for FC1 during experiments (a–d) and simulations (e–h). A blue dye tracer was used in the experiment. In the simulation images, blue denotes the liquid water content at the front grid, while grey denotes that the front grid is dry, but some liquid water is present within the sample at that position. The grey-scale represents the maximum liquid water content for each location. Captured times were at: (a) 20 s, (b) 35 min, (c) 1 hour 25 min, (d) 1 hour 29 min, (e) 20 s, (f) 17 min, (g) 1 hour 19 min, and (h) 1 hour 20 min.
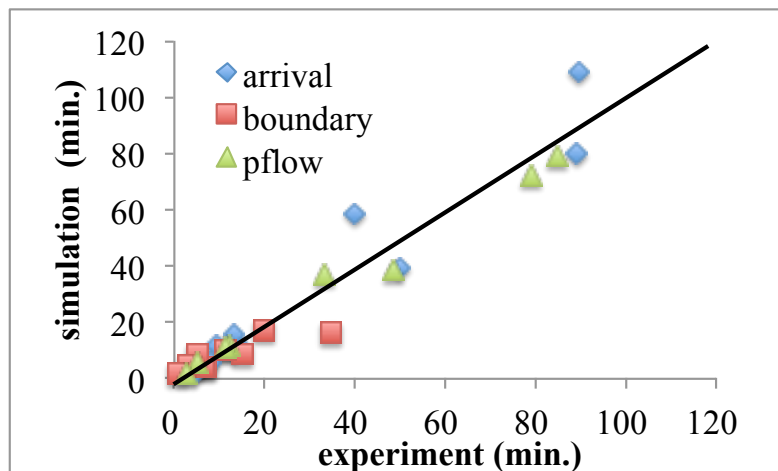
Figure 2: Timings of water arrival at the interface between layers (red squares), formation of preferential flow path (green

5   **triangles), and arrival at snow base (blue diamonds) for experiments and simulations.**
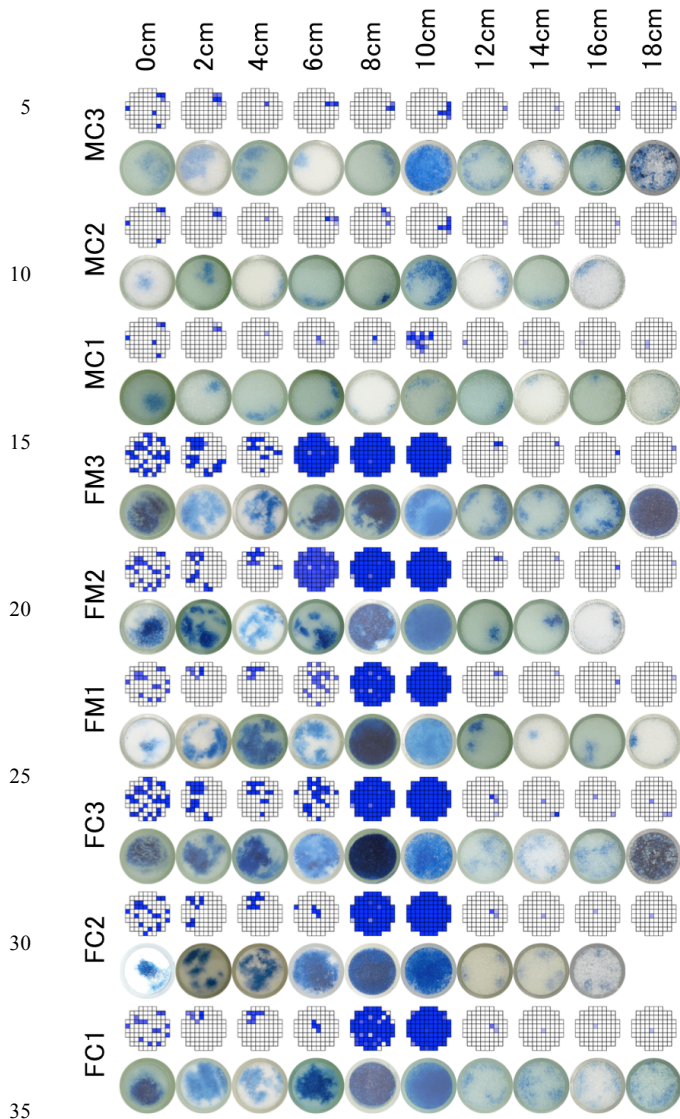
Figure 3: Liquid water distribution (blue shading) at the end of each experiment and simulation. The coordinate on the right denotes the depth of the section from the top surface.
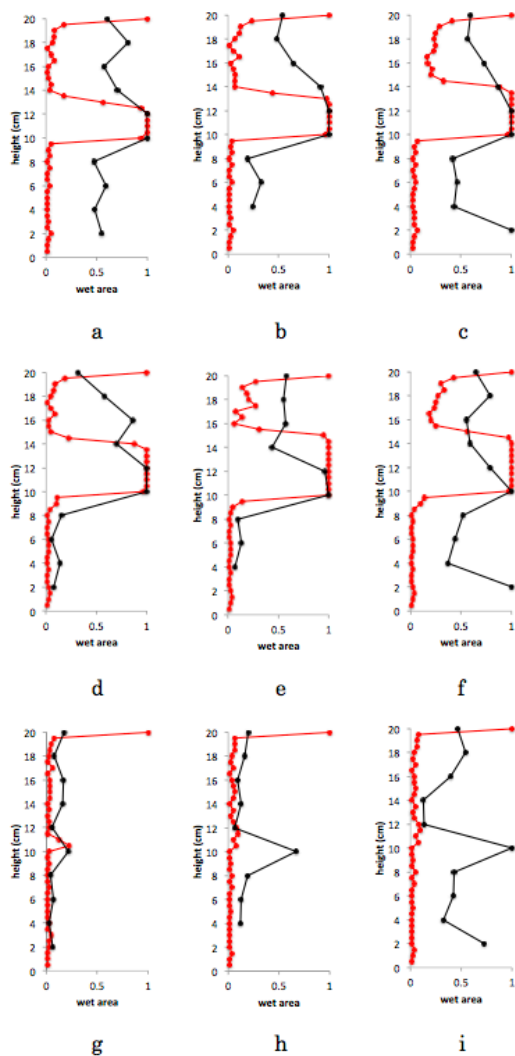
Figure 4: Profiles of wet area for experiments (red line) and simulations (black line): (a) FC1, (b) FC2, (c) FC3, (d) FM1, (e) FM2, (f) FM3, (g) MC1, (h) MC2, and (i) MC3.
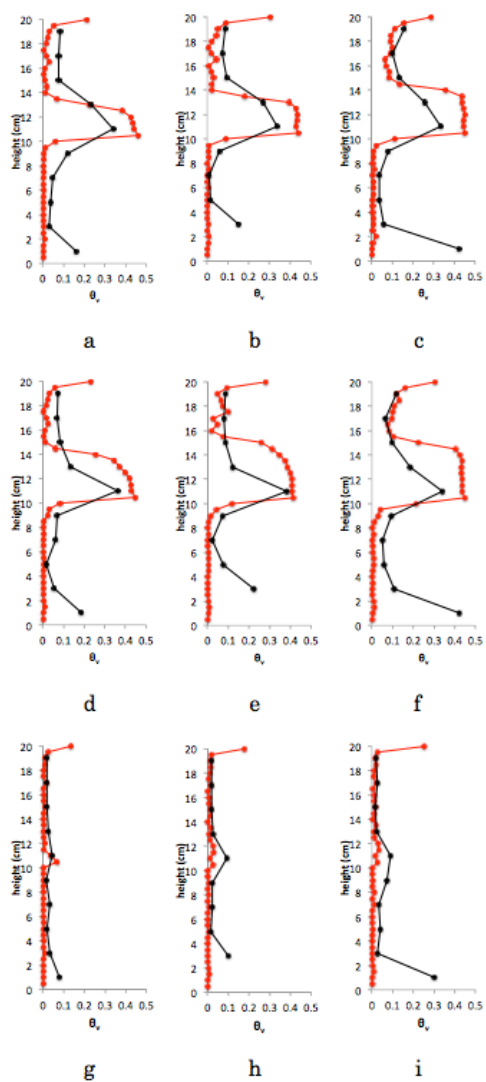
Figure 5: Profiles of volumetric water content for experiments (red line) and simulations (black line): (a) FC1, (b) FC2, (c) FC3, (d) FM1, (e) FM2, (f) FM3, (g) MC1, (h) MC2, (i) MC3.

a   b   c   d
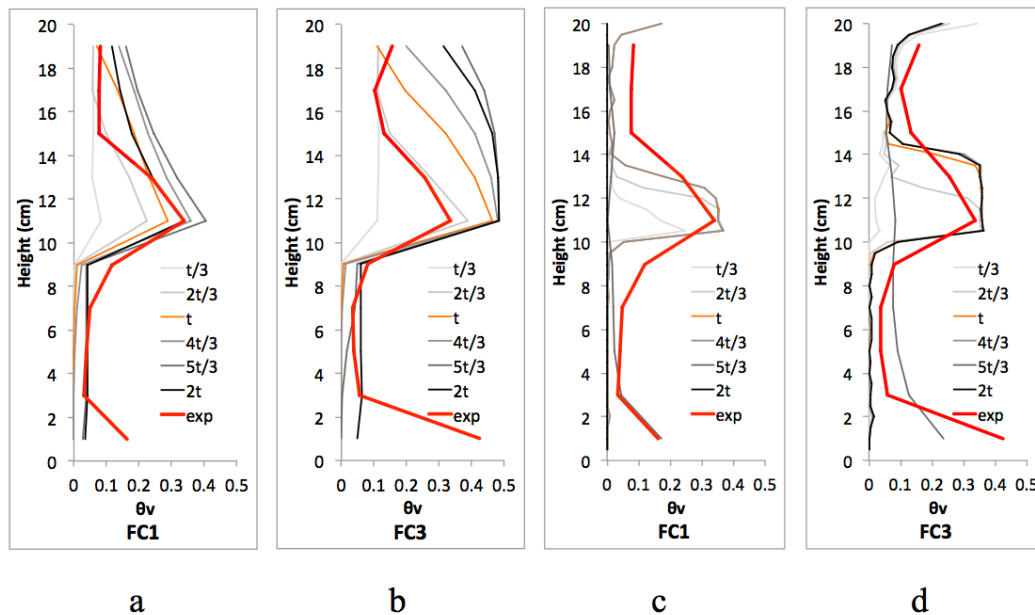
Figure 6: Temporal evolution of simulated water content profiles: (a) FC1 in SNOWPACK, (b) FC3 in SNOWPACK, (c) FC1 in

5 3D model, and (d) FC3 in 3D model. Six profiles are shown in units of the measured arrival time (t).